

## ANNALS OF GLACIOLOGY



**CAMBRIDGE**  
UNIVERSITY PRESS

THIS MANUSCRIPT HAS BEEN SUBMITTED TO THE ANNALS OF GLACIOLOGY AND HAS NOT BEEN PEER-REVIEWED.

**A decade of in situ cosmogenic  $^{14}\text{C}$  in Antarctica**

Journal:	<i>Annals of Glaciology</i>
Manuscript ID	AOG-87-0342.R1
Manuscript Type:	Letter
Date Submitted by the Author:	n/a
Complete List of Authors:	Nichols, Keir; Imperial College London - South Kensington Campus,
Keywords:	Glacial geology, Paleoclimate, Ice chronology/dating
Abstract:	Cosmogenic nuclide measurements in glacial deposits extend our knowledge of glacier chronologies beyond the observational record. The short half-life of in situ cosmogenic $^{14}\text{C}$ makes it particularly useful for studying glacier chronologies, as resulting exposure ages are less sensitive to nuclide inheritance when compared with more commonly measured, long-lived nuclides. An increasing number of laboratories using an automated process to extract carbon from quartz has led to in situ $^{14}\text{C}$ measurements in Antarctic samples at an accelerating rate over the past decade, shedding light on deglaciation in Antarctica. In situ $^{14}\text{C}$ has had the greatest impact in the Weddell Sea Embayment, where inferences on the thickness of ice and timing of deglaciation were limited by inheritance in other cosmogenic nuclide systems. Future subglacial measurements of the nuclide hold much potential as they can provide direct evidence of proposed Holocene thinning and subsequent re-thickening of parts of the Antarctic ice sheets.



SCHOLARONE™  
Manuscripts

1 Title: A decade of in situ cosmogenic  $^{14}\text{C}$  in Antarctica

2

3 Keir Alexander Nichols (contact author)

4 Imperial College London

5 keir.nichols@imperial.ac.uk

6

7

8

9

10

11

12

13

14

15

16

17

18

19

20

21

22

23

24

25

26

27

28

29

30

31

32

33

34

35

36

37

38

39

40

41

42

43

44

45

46

47

48

For Peer Review

**49 ABSTRACT**

50  
51 Cosmogenic nuclide measurements in glacial deposits extend our knowledge of glacier chronologies  
52 beyond the observational record. The short half-life of in situ cosmogenic  $^{14}\text{C}$  makes it particularly useful  
53 for studying glacier chronologies, as resulting exposure ages are less sensitive to nuclide inheritance when  
54 compared with more commonly measured, long-lived nuclides. An increasing number of laboratories  
55 using an automated process to extract carbon from quartz has led to in situ  $^{14}\text{C}$  measurements in Antarctic  
56 samples at an accelerating rate over the past decade, shedding light on deglaciation in Antarctica. In situ  
57  $^{14}\text{C}$  has had the greatest impact in the Weddell Sea Embayment, where inferences on the thickness of ice  
58 and timing of deglaciation were limited by inheritance in other cosmogenic nuclide systems. Future  
59 subglacial measurements of the nuclide hold much potential as they can provide direct evidence of  
60 proposed Holocene thinning and subsequent re-thickening of parts of the Antarctic ice sheets.

**61**  
**62 1. INTRODUCTION**

63  
64 Cosmogenic nuclides are rare nuclides made in near-surface rocks and minerals by cosmic rays. The  
65 concentration of a cosmogenic nuclide in a surface is directly proportional to the time the surface was  
66 most recently uncovered by receding ice. As such, measuring cosmogenic nuclide concentrations is a  
67 common way of studying glacier chronologies (Schaefer and others, 2022). By measuring cosmogenic  
68 nuclides at different elevations above glaciers, we can constrain both the past thickness and timing and  
69 pattern of thinning (Ackert and others, 1999; Stone and others, 2003), typically following the Last Glacial  
70 Maximum (LGM). These geologic constraints are used to validate the results of numerical ice sheet models  
71 investigating deglaciation (e.g., Whitehouse and others, 2012; Pittard and others, 2022), informing model  
72 parameter selection, and ultimately reducing uncertainties when these same models are used to simulate  
73 the future response of ice sheets to a changing climate.

74 Concentrations of cosmogenic nuclides are converted to exposure ages using production rates  
75 and, for radioactive nuclides, their half-lives. Most exposure dating studies use  $^{10}\text{Be}$  or combine it with  
76  $^{26}\text{Al}$  (with half-lives of 1.4 and 0.7 Myr, respectively) (Balco, 2011). Exposure dating studies rely on the  
77 assumption that concentrations accumulated in a single phase of exposure. Cosmogenic nuclides are  
78 predominantly produced in the upper few metres of rock, and we rely on erosion during glaciations to  
79 “reset” surfaces. Preserved beneath cold-based (non-erosive) ice, long-lived nuclides like  $^{10}\text{Be}$  can persist  
80 for multiple glacial-interglacial cycles, breaking the assumption of one period of exposure. Another  
81 cosmogenic nuclide, in situ  $^{14}\text{C}$ , has a much shorter half-life ( $5700 \pm 30$  yr), making concentrations and  
82 resulting exposure ages less sensitive to this nuclide “inheritance”. The half-life is so short that  $^{14}\text{C}$   
83 accumulated prior to the LGM will have decayed away, regardless of how much erosion took place. In situ  
84  $^{14}\text{C}$  exposure ages are therefore essentially free of inheritance, providing unambiguous evidence for the  
85 timing of glacier thinning or retreat.

86 Another useful aspect of in situ  $^{14}\text{C}$  is the potential to constrain the maximum extent of LGM ice.  
87 A balance between production and decay is reached after about 5.5 times the half-life of a radioactive  
88 cosmogenic nuclide, at which point a surface is “saturated”. This means a surface is saturated with in situ  
89  $^{14}\text{C}$  after  $\approx 30$  kyr of exposure, assuming minimal erosion. When we measure a concentration equivalent  
90 to saturation, we know that the sample has been exposed for at least 30 kyr, and thus was not covered  
91 during the LGM. Hence, surfaces saturated with in situ  $^{14}\text{C}$  provide unambiguous evidence for the extent  
92 of ice during the LGM. In summary, in situ  $^{14}\text{C}$  is useful for studying deglaciation because i) concentrations  
93 are essentially uninfluenced by previous periods of exposure, providing exposure ages that are more likely  
94 to reflect the true age of deglaciation when compared with those from long-lived nuclides, and ii)  
95 measurements can provide upper constraints on the extent of ice at the LGM, a type of constraint that

96 cannot be provided by measuring long-lived nuclides. Both of these aspects of in situ  $^{14}\text{C}$  mean measuring  
97 it is particularly useful for benchmarking the results of numerical ice sheet models.

98 A growing number of laboratories capable of extracting in situ  $^{14}\text{C}$  and automation of the  
99 extraction process have led to the nuclide being measured at an enhanced rate over the last decade (Fig.  
100 1a). These measurements are advancing our knowledge of the most recent deglaciation in Antarctica,  
101 especially where inferences from long-lived nuclides are limited. How in situ  $^{14}\text{C}$  is measured, where in  
102 Antarctica it has been measured, and what these measurements have shown us about deglaciation, are  
103 described below. Potential research questions that can be addressed using this nuclide are also outlined,  
104 including estimating glacial erosion rates by combining measurements of in situ  $^{14}\text{C}$  and  $^{10}\text{Be}$ , assessing  
105 the outputs of numerical ice sheet models with single measurements of in situ  $^{14}\text{C}$ , and investigating and  
106 quantifying a proposed Holocene thinning (beneath present) episode with subglacial measurements of in  
107 situ  $^{14}\text{C}$ . Much of our knowledge of the past of the Antarctic ice sheets is based on periods when the ice  
108 sheets were larger than today, such as during the LGM, because evidence for past ice extent is preserved  
109 in rock and sediments above, adjacent to, and offshore of present ice margins. Knowledge of contracted  
110 configurations of the Antarctic ice sheets, gained through subglacial measurements of in situ  $^{14}\text{C}$ , is key to  
111 understanding the future of the ice sheets given that they are predicted to continue losing mass (DeConto  
112 and others, 2021).

113

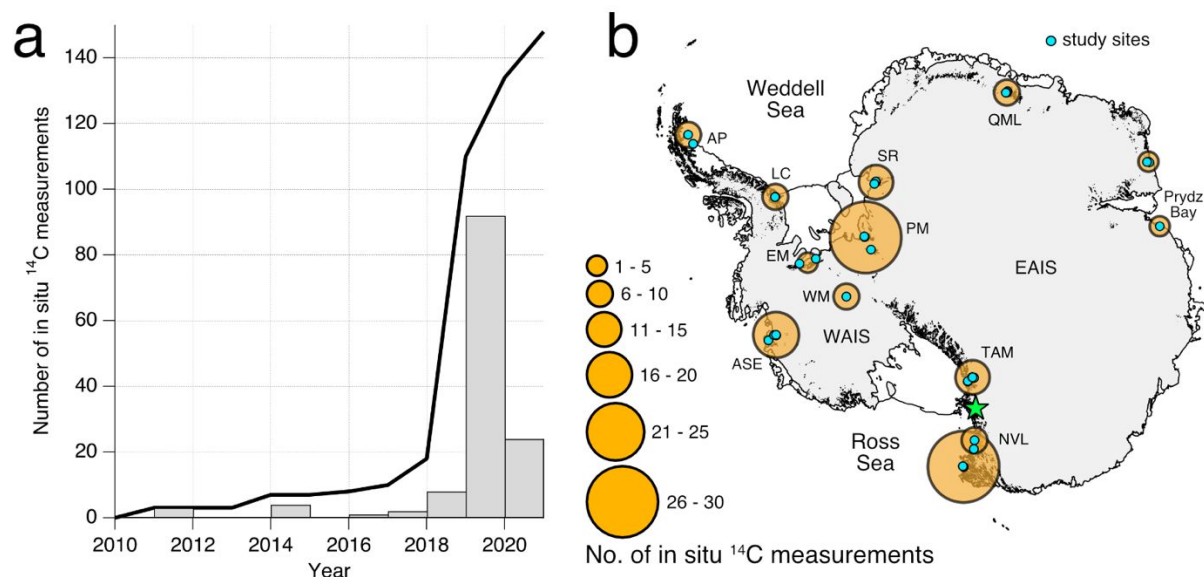
114

## 115 2. HOW IS IN SITU $^{14}\text{C}$ MEASURED?

116

117 The utility of in situ  $^{14}\text{C}$  exposure dating has long been known (e.g., Lal, 1987, 1988; Lal and Jull, 2001) but  
118 it was not until the 2010s that improved reproducibility, increased reliability in extraction systems, and an  
119 accompanying reduction in blank levels, helped make measuring it more routine. Building on methods for  
120 measuring in situ  $^{14}\text{C}$  in extraterrestrial samples (Goel and Kohman, 1962; Suess and Wänke, 1962), Lifton  
121 and others (2001) developed the methods for extracting carbon from quartz used in laboratories today.  
122 Whilst methods differ with laboratory, the key steps are similar: carbon is liberated through the heating  
123 of quartz under vacuum, oxidised to form  $\text{CO}_2$ , then purified using liquid nitrogen. Some extraction lines  
124 use a tube furnace and fuse quartz in a lithium metaborate flux (Lifton and others, 2015; Goehring and  
125 others, 2019a; Lamp and others, 2019), whilst others use an electron bombardment or resistance furnace  
126 to release in situ  $^{14}\text{C}$  by diffusion through the crystal lattice (Fülöp and others, 2015; 2019; Lupker and  
127 others, 2019). Samples are sent for AMS measurement as  $\text{CO}_2$  (Hippe and others, 2013; Lupker and others,  
128 2019) or after dilution and graphitisation (e.g., Lifton and others, 2015). Isotope ratios are used to  
129 determine in situ  $^{14}\text{C}$  concentrations following Hippe and Lifton (2014). In situ  $^{14}\text{C}$  concentrations,  
130 combined with sample density, thickness, elevation, latitude and longitude, and topographic shielding,  
131 are then used to calculate exposure ages, usually using an online exposure age calculator such as the  
132 online calculators formerly known as the CRONUS-Earth online calculators (Balco and others, 2008).

133



134  
135

136 **Fig. 1: a)** Cumulative (black) and yearly (grey bars) total in situ  $^{14}\text{C}$  measurements from Antarctica  
 137 (excluding CRONUS A). **b)** Sampling locations of all published subaerial in situ  $^{14}\text{C}$  measurements from  
 138 Antarctica, excluding those of CRONUS-A (green star). WAIS and EAIS are the West and East Antarctic  
 139 Ice Sheets, respectively. Measurements sourced from the following studies: Antarctic Peninsula (AP), Jeong  
 140 and others (2018), Lassiter Coast (LC), Pensacola Mountains (PM), and Shackleton Range (SR), Nichols and  
 141 others (2019), Ellsworth Mountains (EM), Fogwill and others (2014) and Spector and others (2019),  
 142 Whitmore Mountains (WM), Spector and others (2019), Amundsen Sea Embayment (ASE), Johnson and  
 143 others (2017, 2020), Transantarctic Mountains (TAM), Hillebrand and others (2021), northern Victoria  
 144 Land (NVL), Goehring and others (2019b) and Balco and others (2019), Prydz Bay, Berg and others (2016)  
 145 and White and others (2011), Queen Maud Land (QML), Akçar and others (2020). Map made with  
 146 Quantarctica (Matsuoka and others, 2018).

147  
148

149 The rise in the number of studies applying in situ  $^{14}\text{C}$  (Figure 1a) is fuelled by a number of factors,  
 150 amongst which most notable are a growing number of extraction lines, automation of extraction,  
 151 decreasing blank levels, and the widespread adoption of data reduction and production rate calibration  
 152 methods. Most importantly, an increasing number of laboratories are capable of extracting carbon from  
 153 quartz. Automation of the extraction process has increased sample throughput, particularly at Tulane  
 154 University (Goehring and others, 2019a). A gradual reduction in  $^{14}\text{C}$  in process blanks has improved the  
 155 detection limit. Repeat measurements of the in situ  $^{14}\text{C}$  concentration of the interlaboratory comparison  
 156 material CRONUS-A (Jull and others, 2015) have been used to characterise the reproducibility of in situ  
 157  $^{14}\text{C}$  measurements (approximately 6 %; Nichols and others, 2019) and calibrate the production rate used  
 158 by the online exposure age calculators (Balco and others, 2008) and the Informal Cosmogenic-Nuclide  
 159 Exposure-age Database (ICE-D, [ice-d.org](http://ice-d.org), Balco, 2020). Standardisation of data reduction (Hippe and  
 160 Lifton, 2014) and the identification of a source of contamination from a commonly used method of quartz  
 161 isolation (Nichols and Goehring, 2019) have also contributed to the now relatively routine measurement  
 162 and application of in situ  $^{14}\text{C}$ .

163

### 164 3. ADVANCES BASED ON IN SITU $^{14}\text{C}$

165

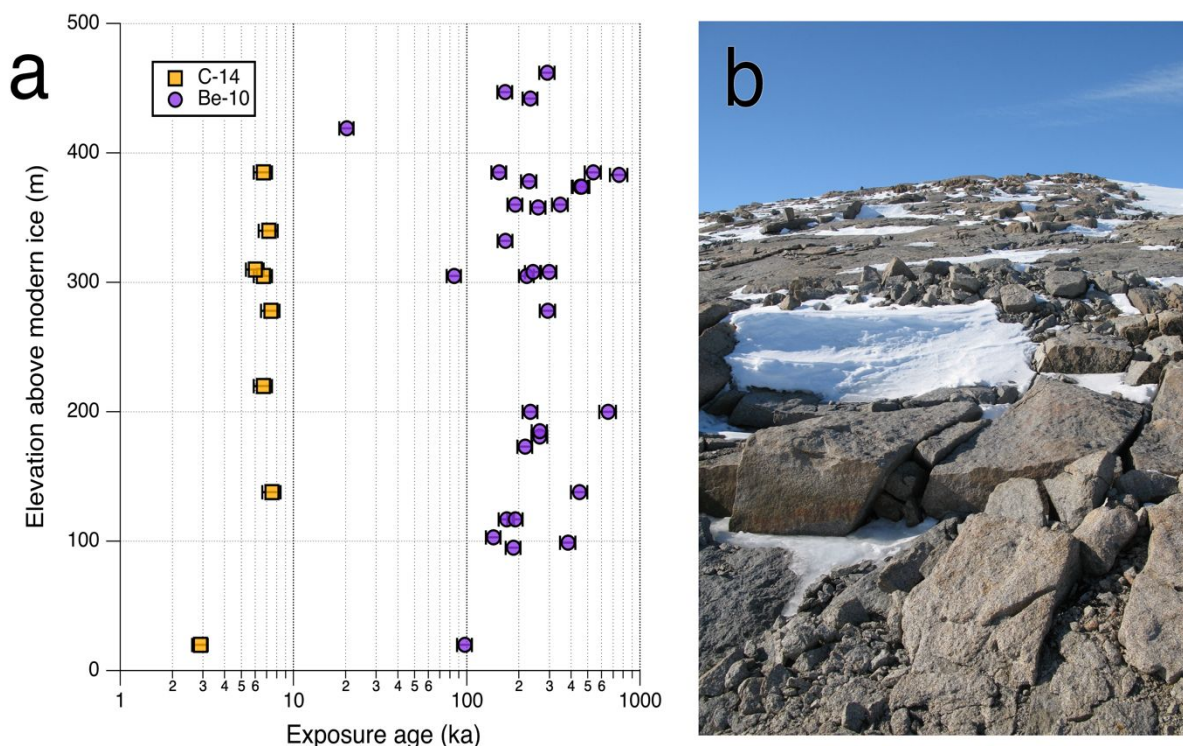
166 Measurements of in situ  $^{14}\text{C}$  are reported from all sectors of Antarctica but are focused in the Ross,  
167 Weddell, and Amundsen sea embayments, with a dearth of measurements in East Antarctica and few on  
168 the Antarctic Peninsula (Fig. 1b). Post-LGM exposure ages constrain deglaciation at most sites, and  
169 saturated measurements constrain the limit of LGM ice in the Shackleton Range (Nichols and others,  
170 2019), close to the West Antarctic Ice Sheet (WAIS) Divide (Spector and others, 2019), and adjacent to  
171 Prydz Bay (Berg and others, 2016). Samples saturated with in situ  $^{14}\text{C}$  are also observed on blue ice  
172 moraines in Queen Maud Land (Akçar and others, 2020). CRONUS-A, a sandstone sample sourced from  
173 1679 m asl in Arena Valley in the Dry Valleys, Antarctica (Jull and others, 2015; Fig. 1b), is saturated with  
174  $^{14}\text{C}$  and has been measured at least 75 times.

175 The most obvious places to measure in situ  $^{14}\text{C}$  for exposure dating studies are those yielding  
176 solely or primarily pre-LGM exposure ages from long-lived nuclides, and thus inferences on the extent of  
177 LGM ice are limited. This is the case at the Lassiter Coast in the Weddell Sea Embayment (Fig. 1b), where  
178 the majority of  $^{10}\text{Be}$  exposure ages of deposits, presumably from the LGM or most recent deglaciation,  
179 exceed 100 ka (Fig. 2a). Taken at face value, one could infer that ice has not been thicker here for hundreds  
180 of thousands of years, certainly not during the LGM. However, in situ  $^{14}\text{C}$  measurements made at the same  
181 site, with many of the same samples, yield Holocene exposure ages (Fig. 2a), showing that i) ice was at  
182 least 380 m thicker than present at the LGM, ii) deglaciation occurred relatively rapidly, and iii) this region  
183 was covered by cold-based ice that preserved  $^{10}\text{Be}$  that accumulated during previous periods of exposure.

184 A similar pattern of pre-LGM  $^{10}\text{Be}$  exposure ages and post-LGM in situ  $^{14}\text{C}$  exposure ages is  
185 observed at other sites in the Weddell Sea Embayment. Limited LGM thickening inferred from  
186 predominantly pre-LGM  $^{10}\text{Be}$  exposure ages in the Shackleton Range (Hein and others, 2011) and  
187 Pensacola Mountains (Balco and others, 2016; Bentley and others, 2017) was used to benchmark ice sheet  
188 models for some time (e.g., Whitehouse and others, 2017; Kingslake and others, 2018). These  
189 interpretations led to relatively little post-LGM ice volume change in the Weddell Sea Embayment (when  
190 compared with previous reconstructions, see Bentley and Anderson (1998)) becoming the predominant  
191 reconstruction amongst the palaeo community (Hillenbrand and others, 2014). Subsequent  
192 measurements of in situ  $^{14}\text{C}$  yielded post-LGM exposure ages at both locations, showing that, rather than  
193 limited thickening, ice was at least 310 and 800 m thicker than present at the LGM (Nichols and others,  
194 2019). Other locations with multiple samples yielding pre-LGM exposure ages from long-lived nuclides  
195 and post-LGM in situ  $^{14}\text{C}$  exposure ages are the Flower Hills and Meyer Hills in the Ellsworth Mountains  
196 (Fogwill and others, 2014) and the Darwin–Hatherton Glacier System in the Ross Sea Embayment  
197 (Hillebrand and others, 2021).

198





199  
 200  
 201 **Fig. 2: a)** Exposure ages from the Lassiter Coast (Nichols and others, 2019; Johnson and others, 2019)  
 202 sourced from ICE-D using the LSDn scaling method. Error bars show external uncertainties but are often  
 203 smaller than symbols. **b)** Collection site of a bedrock sample (P11-11-4) on the Bowman Peninsula, Lassiter  
 204 Coast (Johnson and others, 2019). This bedrock sample has a  $^{10}\text{Be}$  exposure age of  $410 \pm 30$  ka and an in  
 205 situ  $^{14}\text{C}$  exposure age of  $7.4 \pm 0.6$  ka. Photo credit: Joanne Johnson (British Antarctic Survey).  
 206

207 In situ  $^{14}\text{C}$  can also be useful at sites yielding post-LGM  $^{10}\text{Be}$  exposure ages. For example, in the  
 208 Amundsen Sea Embayment, Johnson and others (2020) use measurements of in situ  $^{14}\text{C}$  to identify a  
 209 smaller degree of inheritance in their exposure ages. Here,  $^{10}\text{Be}$  exposure ages ( $n=9$ ) indicate deglaciation  
 210 happened about 17 ka, whilst in situ  $^{14}\text{C}$  exposure ages ( $n=8$ ) show it occurred about 6 ka, a difference of  
 211 11 kyr, which is significant for establishing an accurate deglacial chronology of the region. Samples with  
 212 post-LGM  $^{10}\text{Be}$  exposure ages and younger in situ  $^{14}\text{C}$  exposure ages are also observed at sites in northern  
 213 Victoria Land (Balco and others, 2019; Goehring and others, 2019b), with an additional sample in the  
 214 Flower Hills (Fogwill and others, 2014). Evidently, even when  $^{10}\text{Be}$  exposure ages at a site postdate the  
 215 LGM and thus we know the degree of ice thickness change, there could still be a detectable amount of  
 216 inheritance skewing our understanding of the timing of deglaciation.

217 Glacier chronologies are constrained solely with in situ  $^{14}\text{C}$  measurements (without accompanying  
 218 long-lived nuclides) at some locations, such as the Whitmore Mountains close to WAIS Divide (Spector  
 219 and others, 2019) and some sites in northern Victoria Land (Goehring and others, 2019b). Additionally,  
 220 concordant in situ  $^{14}\text{C}$  and  $^{10}\text{Be}$  exposure ages are observed at many sites in Antarctica (White and others,  
 221 2011; Balco and others, 2019; Goehring and others, 2019b; Hillebrand and others, 2021).  
 222

## 223 4. FUTURE RESEARCH PRIORITIES

### 224 4.1 Measuring in situ $^{14}\text{C}$

225



226  
227 Whilst we have learnt much about deglaciation in Antarctica from in situ  $^{14}\text{C}$  in recent years, we have also  
228 learnt much about measuring the nuclide itself, and some questions remain unanswered. Some studies  
229 observe in situ  $^{14}\text{C}$  concentrations in excess of theoretical limits (Balco and others, 2016; Akçar and others,  
230 2020), whilst another observes measurement reproducibility lower than that expected from  
231 measurement uncertainties alone (Nichols and others, 2019). When sample contamination can be ruled  
232 out, mass movement and supraglacial transport could explain elevated concentrations (Balco and others,  
233 2016), whilst unrecognised measurement error could explain the limited reproducibility. Further work  
234 dedicated to method development is needed to isolate what is i) limiting measurement reproducibility  
235 and ii) contributing toward concentrations exceeding theoretical limits. Most studies measure in situ  $^{14}\text{C}$   
236 in quartz, but the nuclide is produced in other materials such as calcium carbonate (Handwerker and  
237 others, 1999) and olivine (Pigati and others, 2010). Establishing methods for the extraction of carbon from  
238 these materials would expand the number of locations we can study with in situ  $^{14}\text{C}$  beyond only those  
239 rich in quartz.

#### 240 241 **4.2 Applying in situ $^{14}\text{C}$**

242  
243 Further exposure dating studies using in situ  $^{14}\text{C}$  would be useful in areas unstudied with cosmogenic  
244 nuclides or those yielding solely or primarily pre-LGM exposure ages from long-lived nuclides (e.g.,  
245 Hodgson and others 2012). By filling spatial gaps in our knowledge of deglaciation in Antarctica, these  
246 measurements of in situ  $^{14}\text{C}$  would provide more geologic constraints for the benchmarking of numerical  
247 ice sheet models. Additionally, there are a few applications beyond traditional exposure dating yet to be  
248 used (or to their full potential) that could improve our knowledge of the history and glaciology of the  
249 Antarctic ice sheets.

250 How much did glaciers erode into bedrock during the Holocene? This question can be answered  
251 by combining measurements of in situ  $^{14}\text{C}$  and  $^{10}\text{Be}$  in recently exposed proglacial bedrock. Making direct  
252 measurements of subglacial erosion is complicated by the difficulty of accessing the beds of glaciers. Using  
253 cosmogenic nuclides to estimate past erosion rates provides knowledge of glacial processes over a longer  
254 period than contemporary point measurements, extending our knowledge of glacial erosion rates beyond  
255 the observational record. The relationship between the in situ  $^{14}\text{C}$  and  $^{10}\text{Be}$  concentration of a proglacial  
256 bedrock sample is related to the depth to which a glacier eroded into bedrock in the Holocene, allowing  
257 the estimation of Holocene glacial erosion rates (Rand and Goehring, 2019). Because this method requires  
258 proglacial bedrock, it may be limited to smaller glaciers such as those on the Antarctic Peninsula or at high  
259 elevations on the continent.

260 How closely do numerical ice sheet model outputs reflect the timing of both the advance and  
261 retreat phases of deglaciation contained in geologic archives? Measurements of in situ  $^{14}\text{C}$ , rather than  
262 long-lived nuclides, can answer this question. Many numerical ice sheet models are benchmarked against  
263 exposure age datasets recording only deglaciation. By assuming samples were saturated prior to LGM  
264 burial, individual measurements of in situ  $^{14}\text{C}$  can be used to assess the timing of both advance and retreat  
265 phases of model outputs (Spector and others, 2019), reducing uncertainties when these same models are  
266 used to simulate the future of ice sheets. More generally, targeting exposed surfaces high above modern  
267 ice elevations could help provide more upper constraints on LGM ice thicknesses to help validate  
268 numerical ice sheet model outputs.

269 To what extent, and where, did parts of the Antarctic ice sheets readvance in the Holocene? This  
270 is perhaps the most important question that in situ  $^{14}\text{C}$  can answer. A number of studies, both through  
271 geologic observations (Siegert and others, 2013; Wolstencroft and others, 2015; Greenwood and others,  
272 2018; King and others, 2022) and modelling (Kingslake and others, 2018), infer that some parts of the the  
273 Antarctic ice sheets were smaller than present in the Holocene and subsequently grew to their present

274 configuration. Through measuring carbon in subglacial sediments, two studies (Venturelli and others,  
275 2020 and Neuhaus and others, 2021) report the first direct evidence of a Holocene grounding line  
276 readvance in the Ross sector. Further direct evidence for a Holocene readvance can be obtained through  
277 in situ  $^{14}\text{C}$  measurements in subglacial bedrock, because significant concentrations in subglacial bedrock  
278 unambiguously requires Holocene exposure, either complete or through relatively thin ice (Johnson and  
279 others, 2022). Constraining the scale of this readvance, both in ice thickness change and geographic  
280 extent, could shed light on the processes causing the mass loss and subsequent gain (e.g., ocean forcings,  
281 glacioisostatic adjustment), information that can then be used with numerical models to replicate this ice  
282 sheet behaviour. Given that current Antarctic ice sheet mass loss is predicted to continue (DeConto and  
283 others, 2021), knowing the processes that helped recover ice mass loss in a climate relatively similar to  
284 that of today is key to understanding the reversibility of current and future Antarctic ice mass loss. Whilst  
285 previous studies have investigated long term changes in the Greenland Ice Sheet by measuring long-lived  
286 nuclides in subglacial material (Schaefer and others, 2016; Christ and others, 2021), there are no published  
287 subglacial measurements of in situ  $^{14}\text{C}$  from beneath any ice sheet. If above background in situ  $^{14}\text{C}$   
288 indicative of a Holocene readvance is measured in samples collected from beneath the Antarctic ice  
289 sheets, multiple studies will be required to confirm if this ice sheet behaviour is widespread or localised.

290

## 291 5. CONCLUSIONS

292

293 To summarise, the cosmogenic nuclide in situ  $^{14}\text{C}$  has been measured at an enhanced rate over the last  
294 decade, fuelled by the automation of the extraction process and an increasing number of laboratories  
295 now capable of extracting it. Measurements of in situ  $^{14}\text{C}$  have been used in exposure dating studies to  
296 shed light on deglaciation in all sectors of Antarctica, but especially in the Weddell Sea Embayment. Some  
297 studies observe in situ  $^{14}\text{C}$  concentrations exceeding theoretical limits and also measurement  
298 reproducibility lower than expected, which can hopefully be addressed with dedicated work on  
299 understanding the extraction process and geomorphic scatter. Whilst there are many locations in  
300 Antarctica where traditional in situ  $^{14}\text{C}$  exposure dating studies would be useful, there are also a number  
301 of other applications of the nuclide that hold much potential, including using subglacial measurements to  
302 constrain episodes of thinning and rethickening in the Holocene.

303

304

## 305 REFERENCES

306

- 307 Akçar, N and 6 others (2020) Build-up and chronology of blue ice moraines in Queen Maud Land,  
308 Antarctica, *Quaternary Science Advances*, 2(May), 100012 (doi:10.1016/j.qsa.2020.100012)
- 309 Ackert, RP Jr and 6 others (1999) Measurements of Past Ice Sheet Elevations in Interior West Antarctica,  
310 *Science*, 286 (5438), 276-280 (doi:10.1126/science.286.5438.27)
- 311 Balco, G (2020) Technical note: A prototype transparent-middle-layer data management and analysis  
312 infrastructure for cosmogenic-nuclide exposure dating, *Geochronology*, 2, 169–175  
313 (doi:10.5194/gchron-2020-6)
- 314 Balco, G (2011) Contributions and unrealized potential contributions of cosmogenic-nuclide exposure  
315 dating to glacier chronology, 1990-2010, *Quaternary Science Reviews*, 30(1–2), 3–27  
316 (doi:10.1016/j.quascirev.2010.11.003)
- 317 Balco, G, Todd, C, Goehring, BM, Moening-Swanson, I and Nichols, K (2019) Glacial geology and  
318 cosmogenic-nuclide exposure ages from the Tucker Glacier - Whitehall Glacier confluence, northern  
319 Victoria Land, Antarctica, *American Journal of Science*, 319(April), 255–286 (doi:10.2475/04.2019.01)

- 320 Balco, G and 7 others (2016) Cosmogenic-nuclide exposure ages from the Pensacola Mountains adjacent  
321 to the foundation ice stream, Antarctica, *American Journal of Science*, 316, 542–577  
322 (doi.org/10.2475/06.2016.02)
- 323 Balco, G, Stone, JO, Lifton, NA and Dunai, TJ (2008) A complete and easily accessible means of  
324 calculating surface exposure ages or erosion rates from  $^{10}\text{Be}$  and  $^{26}\text{Al}$  measurements, *Quaternary*  
325 *Geochronology*, 3(3), 174–195 (doi:10.1016/j.quageo.2007.12.001)
- 326 Bentley, MJ and Anderson, JB (1998) Glacial and marine geological evidence for the ice sheet  
327 configuration in the Weddell Sea–Antarctic Peninsula region during the Last Glacial Maximum, *Antarctic*  
328 *Science*, 10(3), 309–325 (doi:10.1017/s0954102098000388)
- 329 Bentley, MJ and 6 others (2017) Deglacial history of the Pensacola Mountains, Antarctica from glacial  
330 geomorphology and cosmogenic nuclide surface exposure dating, *Quaternary Science Reviews*, 158, 58–  
331 76 (doi:10.1016/j.quascirev.2016.09.028)
- 332 Berg, S and 6 others (2016) Unglaciaded areas in East Antarctica during the Last Glacial (Marine Isotope  
333 Stage 3) – New evidence from Rauer Group, *Quaternary Science Reviews*, 153, 1–10  
334 (doi:10.1016/j.quascirev.2016.08.021)
- 335 Christ, AJ and 17 others (2021) A multimillion-year-old record of Greenland vegetation and glacial  
336 history preserved in sediment beneath 1.4 km of ice at Camp Century, *Proceedings of the National*  
337 *Academy of Sciences*, 118(13) (doi:10.1073/pnas.2021442118)
- 338 DeConto, RM and 12 others (2021) The Paris Climate Agreement and future sea-level rise from  
339 Antarctica, *Nature*, 593, 83–89 (doi:10.1038/s41586-021-03427-0)
- 340 Fogwill, CJ and 8 others (2014) Drivers of abrupt Holocene shifts in West Antarctic ice stream direction  
341 determined from combined ice sheet modelling and geologic signatures, *Antarctic Science*, 26(6), 674–  
342 686 (doi:10.1017/S0954102014000613)
- 343 Fülöp, RH and 7 others (2019) The ANSTO – University of Wollongong in-situ  $^{14}\text{C}$  extraction laboratory,  
344 *Nuclear Instruments and Methods in Physics Research Section B: Beam Interactions with Materials and*  
345 *Atoms*, 438(April 2018), 207–213 (doi:10.1016/j.nimb.2018.04.018)
- 346 Fülöp, RH, Wacker, L and Dunai, TJ (2015) Progress report on a novel in situ  $^{14}\text{C}$  extraction scheme at  
347 the University of Cologne, *Nuclear Instruments and Methods in Physics Research Section B: Beam*  
348 *Interactions with Materials and Atoms*, 361, 20–24 (doi:10.1016/j.nimb.2015.02.023)
- 349 Goehring, BM, Wilson, J and Nichols, K (2019a) A fully automated system for the extraction of in situ  
350 cosmogenic carbon-14 in the Tulane University cosmogenic nuclide laboratory, *Nuclear Instruments and*  
351 *Methods in Physics Research Section B: Beam Interactions with Materials and Atoms*, 455, 284–292  
352 (doi:10.1016/j.nimb.2019.02.006)
- 353 Goehring, BM, Balco, G, Todd, C, Moening-Swanson, I and Nichols, K (2019b) Late-glacial grounding line  
354 retreat in the northern Ross Sea, Antarctica, *Geology*, 47(4), 1–4 (doi:10.1130/G45413.1)
- 355 Goel, PS, Kohman, PK (1962) Cosmogenic Carbon-14 in Meteorites and Terrestrial Ages of “Finds” and  
356 Craters, *Science*, 136(3519), 875–876
- 357 Greenwood, SL, Simkins, LM, Halberstadt, ARW, Prothro, LO and Anderson, JB (2018) Holocene  
358 reconfiguration and readvance of the East Antarctic Ice Sheet, *Nature Communications*, 9(1)  
359 (doi:10.1038/s41467-018-05625-3)
- 360 Handwerker, DA, Cerling, TE and Bruhn, RL (1999) Cosmogenic  $^{14}\text{C}$  in carbonate rocks, *Geomorphology*,  
361 27(1–2), 13–24 (doi:10.1016/S0169-555X(98)00087-7)
- 362 Hein, AS, Fogwill, CJ, Sugden, DE and Xu, S (2011) Glacial/interglacial ice-stream stability in the Weddell  
363 Sea embayment, Antarctica, *Earth and Planetary Science Letters*, 307(1–2), 211–221  
364 (doi:10.1016/j.epsl.2011.04.037)
- 365 Hillebrand, TR and 8 others (2021) Holocene thinning of Darwin and Hatherton glaciers, Antarctica, and  
366 implications for grounding-line retreat in the Ross Sea, *Cryosphere*, 15(7), 3329–3354 (doi:10.5194/tc-  
367 15-3329-2021)

- 368 Hillenbrand, CD and 14 others (2014) Reconstruction of changes in the Weddell Sea sector of the  
369 Antarctic Ice Sheet since the Last Glacial Maximum, *Quaternary Science Reviews*, 100, 111–136  
370 (doi:10.1016/j.quascirev.2013.07.020)
- 371 Hippe, K and Lifton, NA (2014) Calculating Isotope Ratios and Nuclide Concentrations for In Situ  
372 Cosmogenic  $^{14}\text{C}$  Analyses, *Radiocarbon*, 56(03), 1167–1174 (doi:10.2458/56.17917)
- 373 Hippe, K and 7 others (2013) An update on in situ cosmogenic  $^{14}\text{C}$  analysis at ETH Zürich, *Nuclear  
374 Instruments and Methods in Physics Research Section B: Beam Interactions with Materials and Atoms*,  
375 294, 81–86 (doi:10.1016/j.nimb.2012.06.020)
- 376 Hodgson, DA and 6 others (2012) Glacial geomorphology and cosmogenic  $^{10}\text{Be}$  and  $^{26}\text{Al}$  exposure ages  
377 in the northern Dufek Massif, Weddell Sea embayment, Antarctica, *Antarctic Science*, 24(4), 377–394  
378 (doi:10.1017/S0954102012000016)
- 379 Jeong, A and 8 others (2018) Late Quaternary deglacial history across the Larsen B embayment,  
380 Antarctica, *Quaternary Science Reviews*, 189, 134–148 (doi:10.1016/j.quascirev.2018.04.011)
- 381 Johnson, JS and 12 others (2022) Review article: Existing and potential evidence for Holocene grounding  
382 line retreat and readvance in Antarctica, *Cryosphere*, 16(5), 1543–1562 (doi:10.5194/tc-16-1543-2022)
- 383 Johnson, JS and 10 others (2020) Deglaciation of Pope Glacier implies widespread early Holocene ice  
384 sheet thinning in the Amundsen Sea sector of Antarctica, *Earth and Planetary Science Letters*, 548,  
385 116501 (doi:10.1016/j.epsl.2020.116501)
- 386 Johnson, JS, Nichols, KA, Goehring, BM, Balco, G and Schaefer, JM (2019) Abrupt mid-Holocene ice loss  
387 in the western Weddell Sea Embayment of Antarctica, *Earth and Planetary Science Letters*, 518, 127–135  
388 (doi:10.1016/j.epsl.2019.05.002)
- 389 Johnson, JS and 8 others (2017) The last glaciation of Bear Peninsula, central Amundsen Sea Embayment  
390 of Antarctica: Constraints on timing and duration revealed by in situ cosmogenic  $^{14}\text{C}$  and  $^{10}\text{Be}$  dating,  
391 *Quaternary Science Reviews*, 178, 77–88 (doi:10.1016/j.quascirev.2017.11.003)
- 392 Jull, AJT, Scott, EM and Bierman, P (2015) The CRONUS-Earth inter-comparison for cosmogenic isotope  
393 analysis, *Quaternary Geochronology*, 26(1), 3–10 (doi:10.1016/j.quageo.2013.09.003)
- 394 King, MA, Watson, CS and White, D (2022) GPS Rates of Vertical Bedrock Motion Suggest Late Holocene  
395 Ice-Sheet Readvance in a Critical Sector of East Antarctica, *Geophysical Research Letters*, 49(4)  
396 (doi:10.1029/2021GL097232)
- 397 Kingslake, J and 9 others (2018) Extensive retreat and re-advance of the West Antarctic Ice Sheet during  
398 the Holocene, *Nature*, 558(7710), 430–434 (doi:10.1038/s41586-018-0208-x)
- 399 Lal, D and Jull, AJT (2001) In-situ cosmogenic  $^{14}\text{C}$ : Production and examples of its unique applications in  
400 studies of terrestrial and extraterrestrial processes, *Radiocarbon*, 43(2B), 731–742  
401 (doi:10.1017/s0033822200041394)
- 402 Lal, D (1988) In situ produced cosmogenic isotopes in terrestrial rocks, *Annual Review of Earth and  
403 Planetary Sciences*, 16, 355–388
- 404 Lal, D (1987) Cosmogenic nuclides produced in situ in terrestrial solids, *Nuclear Instruments and  
405 Methods in Physics Research Section B: Beam Interactions with Materials and Atoms*, 29(1-2), 238–245
- 406 Lamp, JL and 6 others (2019) Update on the cosmogenic in situ  $^{14}\text{C}$  laboratory at the Lamont-Doherty  
407 Earth Observatory, *Nuclear Instruments and Methods in Physics Research Section B: Beam Interactions  
408 with Materials and Atoms*, (April), 1–6 (doi:10.1016/j.nimb.2019.05.064)
- 409 Lifton, NA, Jull, AJT and Quade, J (2001) A new extraction technique and production rate estimate for in  
410 situ cosmogenic  $^{14}\text{C}$  in quartz, *Geochimica et Cosmochimica Acta*, 65(12), 1953–1969  
411 (doi:10.1016/S0016-7037(01)00566-X)
- 412 Lifton, N, Goehring, B, Wilson, J, Kubley, T and Caffee, M (2015) Progress in automated extraction and  
413 purification of in situ  $^{14}\text{C}$  from quartz: Results from the Purdue in situ  $^{14}\text{C}$  laboratory, *Nuclear  
414 Instruments and Methods in Physics Research Section B: Beam Interactions with Materials and Atoms*,  
415 361, 381–386 (doi:10.1016/j.nimb.2015.03.028)



- 416 Lupker, M and 7 others (2019) In-situ cosmogenic  $^{14}\text{C}$  analysis at ETH Zürich: Characterization and  
417 performance of a new extraction system, *Nuclear Instruments and Methods in Physics Research Section*  
418 *B: Beam Interactions with Materials and Atoms*, 457(July), 30–36 (doi:10.1016/j.nimb.2019.07.028)
- 419 Matsuoka, K, Skoglund, A, and Roth, G (2018) Quantarctica [Data set]. Norwegian Polar Institute  
420 (doi.org/10.21334/npolar.2018.8516e961)
- 421 Neuhaus, SU, and 6 others (2021) Did Holocene climate changes drive West Antarctic grounding line  
422 retreat and readvance?, *Cryosphere*, 15(10), 4655–4673 (doi:10.5194/tc-15-4655-2021)
- 423 Nichols, KA and Goehring, BM (2019) Isolation of quartz for cosmogenic in situ  $^{14}\text{C}$  analysis,  
424 *Geochronology*, 1(1), 43–52 (doi:10.5194/gchron-1-43-2019)
- 425 Nichols, KA, Goehring, BM, Balco, G, Johnson, JS, Hein, AS and Todd, C (2019) New Last Glacial Maximum  
426 ice thickness constraints for the Weddell Sea Embayment, Antarctica, *Cryosphere*, 13, 2935–2951  
427 (doi:10.5194/tc-13-2935-2019)
- 428 Pigati, JS, Lifton, NA, Jull, AJT and Quade, J (2010) Extraction of in situ cosmogenic  $^{14}\text{C}$  from Olivine,  
429 *Radiocarbon*, 52(3), 1244–1260 (doi:10.1017/S0033822200046336)
- 430 Pittard, ML, Whitehouse, PL, Bentley, MJ, Small, D (2022) An ensemble of Antarctic deglacial simulations  
431 constrained by geological observations, *Quaternary Science Reviews*, 298  
432 ([doi:10.1016/j.quascirev.2022.107800](https://doi.org/10.1016/j.quascirev.2022.107800))
- 433 Rand, C and Goehring, BM (2019) The distribution and magnitude of subglacial erosion on millennial  
434 timescales at Engabreen, Norway, *Annals of Glaciology*, 60(80), 73–81 (doi:10.1017/aog.2019.42)
- 435 Schaefer, JM and 6 others (2022) Cosmogenic nuclide techniques, *Nature Reviews Methods Primers*, 2(1)  
436 (doi:10.1038/s43586-022-00096-9)
- 437 Schaefer, JM and 8 others (2016) Greenland was nearly ice-free for extended periods during the  
438 Pleistocene, *Nature*, 540(7632), 252–255 (doi:10.1038/nature20146)
- 439 Siegert, M, Ross, N, Corr, H, Kingslake, J and Hindmarsh, R (2013) Late Holocene ice-flow reconfiguration  
440 in the Weddell Sea sector of West Antarctica, *Quaternary Science Reviews*, 78, 98–107  
441 (doi:10.1016/j.quascirev.2013.08.003)
- 442 Spector, P, Stone, J and Goehring, B (2019) Thickness of the divide and flank of the West Antarctic Ice  
443 Sheet through the last deglaciation, *Cryosphere*, 13(11), 3061–3075 (doi:10.5194/tc-13-3061-2019)
- 444 Suess, HE, Wänke, H (1962) Radiocarbon content and terrestrial age of twelve stony meteorites and one  
445 iron meteorite, *Geochimica et Cosmochimica Acta*, 26, 475–480
- 446 Stone, JO and 6 others (2003) Holocene Deglaciation of Marie Byrd Land, West Antarctica, *Science*, 299  
447 (5603), 99–102 (doi:10.1126/science.1077998)
- 448 Venturelli, RA and 9 others (2020) Mid-Holocene Grounding Line Retreat and Readvance at Whillans Ice  
449 Stream, West Antarctica, *Geophysical Research Letters*, 47(15), 0–2 (doi:10.1029/2020GL088476)
- 450 White, D, Fülöp, RH, Bishop, P, Mackintosh, A and Cook, G (2011) Can in-situ cosmogenic  $^{14}\text{C}$  be used to  
451 assess the influence of clast recycling on exposure dating of ice retreat in Antarctica?, *Quaternary*  
452 *Geochronology*, 6(3–4), 289–294 (doi:10.1016/j.quageo.2011.03.004)
- 453 Whitehouse, PL, Bentley, MJ and Le Brocq, AM (2012) A deglacial model for Antarctica: geological  
454 constraints and glaciological modelling as a basis for a new model of Antarctic glacial isostatic  
455 adjustment, *Quaternary Science Reviews*, 32, 1–24 (doi:10.1016/j.quascirev.2011.11.016)
- 456 Whitehouse, PL, Bentley, MJ, Vieli, A, Jamieson, SSR, Hein, AS, and Sugden, DE (2017) Controls on Last  
457 Glacial Maximum ice extent in the Weddell Sea embayment, Antarctica, *Journal of Geophysical Research*  
458 *Earth Surface*, 122, 371–397 (doi.org/10.1002/2016JF004121)
- 459 Wolstencroft, M and 12 others (2015) Uplift rates from a new high-density GPS network in Palmer Land  
460 indicate significant late Holocene ice loss in the southwestern Weddell Sea, *Geophysical Journal*  
461 *International*, 203(1), 737–754 (doi:10.1093/gji/ggv327)

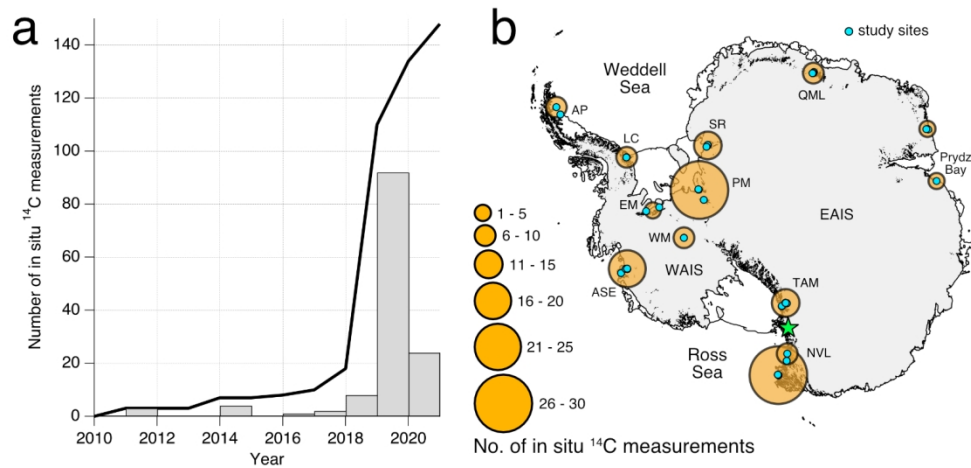


Fig. 1: a) Cumulative (black) and yearly (grey bars) total in situ  $^{14}\text{C}$  measurements from Antarctica (excluding CRONUS A). b) Sampling locations of all published subaerial in situ  $^{14}\text{C}$  measurements from Antarctica, excluding those of CRONUS-A (green star). WAIS and EAIS are the West and East Antarctic Ice Sheets, respectively. Measurements sourced from the following studies: Antarctic Peninsula (AP), Jeong and others (2018), Lassiter Coast (LC), Pensacola Mountains (PM), and Shackleton Range (SR), Nichols and others (2019), Ellsworth Mountains (EM), Fogwill and others (2014) and Spector and others (2019), Whitmore Mountains (WM), Spector and others (2019), Amundsen Sea Embayment (ASE), Johnson and others (2017, 2020), Transantarctic Mountains (TAM), Hillebrand and others (2021), northern Victoria Land (NVL), Goehring and others (2019b) and Balco and others (2019), Prydz Bay, Berg and others (2016) and White and others (2011), Queen Maud Land (QML), Akçar and others (2020). Map made with Quantarctica (Matsuoka and others, 2018).

358x175mm (118 x 118 DPI)



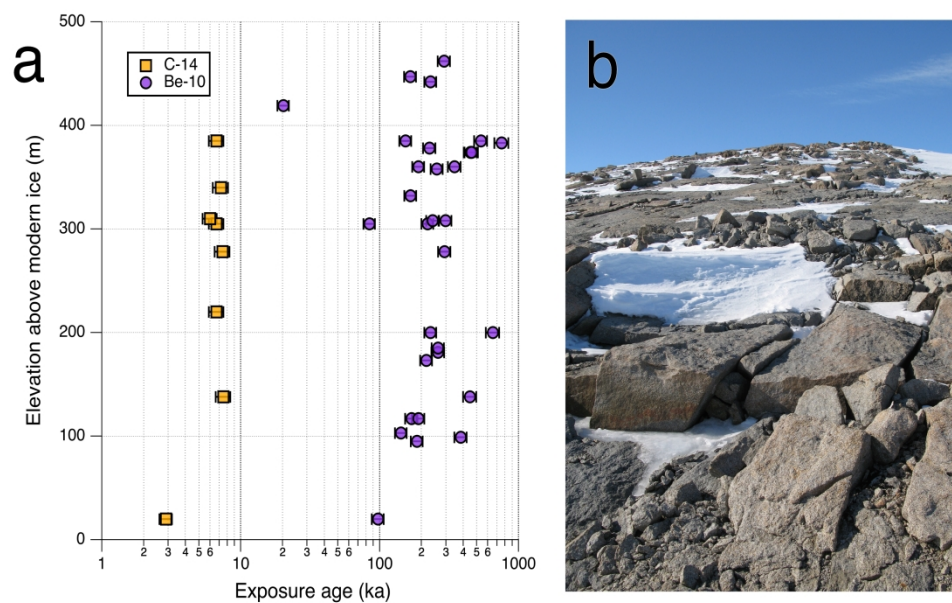


Fig. 2: a) Exposure ages from the Lassiter Coast (Nichols and others, 2019; Johnson and others, 2019) sourced from ICE-D using the LSDn scaling method. Error bars show external uncertainties but are often smaller than symbols. b) Collection site of a bedrock sample (P11-11-4) on the Bowman Peninsula, Lassiter Coast (Johnson and others, 2019). This bedrock sample has a  $^{10}\text{Be}$  exposure age of  $410 \pm 30$  ka and an in situ  $^{14}\text{C}$  exposure age of  $7.4 \pm 0.6$  ka. Photo credit: Joanne Johnson (British Antarctic Survey).

851x534mm (118 x 118 DPI)